Extremely low-frequency phonon material and its temperature- and photo-induced switching effects

Takaya Yoshida,[1] Koji Nakabayashi,[1] Hiroko Tokoro,[1,2] Marie Yoshikiyo,[1]
Asuka Namai,[1] Kenta Imoto,[1] Kouji Chiba,[3] and Shin-ichi Ohkoshi*[,1]

[1] *Department of Chemistry, School of Science, The University of Tokyo*
7-3-1 Hongo, Bunkyo-ku, Tokyo 113-0033, Japan.
[2] *Division of Materials Science, Faculty of Pure and Applied Sciences, University of Tsukuba*
1-1-1 Tennodai, Tsukuba, Ibaraki 305-8573, Japan.
[3] *Material Science Div., MOLSIS Inc., Tokyo Daia Bldg.*
1-28-38 Shinkawa, Chuo-ku, Tokyo 104-0033, Japan.

*To whom correspondence should be addressed
E-mail: ohkoshi@chem.s.u-tokyo.ac.jp

Table of Contents: **Page**

1	Legend for Supporting Movies	S2
2	Experimental details	S3
3	Crystal structure analysis of Co^{II}–W^{V} phase of **RbCoW** (Table S1)	S4
4	First-principles phonon mode calculation (Table S2-S4, Figure S1)	S5–S8
5	Temperature-induced switching effect on the low-frequency phonon mode (Figure S2)	S9
6	Crystal structure analysis of the Co^{III}–W^{IV} phase of **RbCoW** (Figure S3, Table S5)	S10,S11
7	Comparison of the crystal structure of **RbCoW** between the Co^{II}–W^{V} phase and Co^{III}–W^{IV} phase (Tables S6, S7)	S12
8	First-principles electronic structure calculation of the Co^{III}–W^{IV} phase (Figure S4)	S13
9	THz absorption spectrum of **CsCoW** (Figure S5)	S14

Section 1. Legend for Supporting Movies

Movie S1. "Low-frequency phonon millefeuille" based on metal–organic framework. Initial part of the movie shows monoatomic molecules shown with red balls moving freely in the gas phase or liquid phase (translational mode). Next, a monoatomic molecule is caught by a two-dimensional (2D) metal–organic soft framework (similar to pastry sheets), and the translational mode switches to a vibrational mode (optical phonon mode) with a low vibrational frequency. The layers pile up with the 2D layers softly sandwiching the low-frequency optical phonon due to heavy atoms. Here we call it "low-frequency phonon millefeuille".

Movie S2. Calculated phonon modes of RbCoW. The first part of the movie shows the list of low-frequency optical phonon modes. Then, the movie shows the atomic movements of the phonon modes corresponding to **peaks a** (0.883 THz), **b** (0.997 THz), **c** (1.136 THz), **d** (1.453 THz), **e** (1.682 THz), **f** (1.805 THz), **g** (1.923 THz), and **h** (2.102 THz) in the optical phonon spectrum. **Peaks a**, **b** and **c** are assigned to the phonon modes of Rb ion vibrations in the *ab* plane. Atomic movement of **peak d** is due to Rb ion oscillation along the crystallographic *c*-axis. In these phonon modes, the 3-cyanopyridine and cyanide ligands sway together with the Rb ions, supporting the Rb movements. **Peaks e** and **f** are attributed to the combination of transverse translational modes of W–CN–Co and 3-cyanopyridine ligand rotation, and **peaks g** and **h** originate from the transverse librational modes of W–CN–Co and 3-cyanopyridine ligand rotation. Red, blue, green, ocher, and grey balls represent Rb, Co, W, C, and N atoms, respectively.

Section 2. Experimental details

Synthesis. Polycrystalline sample of **RbCoW** was synthesised by reacting a 15 mL aqueous solution of cobalt (II) dichloride (2.3 mmol), 3-cyanopyridine (3.0 mmol), rubidium chloride (7.6 mmol) with a 15 mL solution of rubidium octacyanidetungstate hydrate (1.5 mmol) and rubidium chloride (0.45 mol dm^{-3}). Stirring for 24 hours and subsequently standing under vacuum conditions at room temperature yielded a red-brown powder.

Measurements. The chemical formulas of the metal assemblies were estimated by micro-analytical methods for carbon, nitrogen, and hydrogen. The chemical composition of the metal ions (Rb, Co, W) were estimated by inductively coupled plasma mass spectroscopy using Agilent 7700x. Infrared absorption spectrum of **RbCoW** was obtained by JASCO FT/IR-4100 and Shimadzu FTIR-8200 spectrometers. The sample was prepared by standing under an Ar atmosphere, dispersing with nujol, and sandwiching between CaF_2 plates. UV-visible absorption spectra of **RbCoW** were obtained by Shimadzu 3600 Plus. The sample was prepared by standing under an Ar atmosphere, dispersing with nujol, and sandwiching between polypropylene plates. The temperature-dependent spectra of UV-vis absorption were obtained using Oxford MicrostatHe2. Additionally, 785 nm CW laser (48.5 mW) made by Applied Techno was used for photo-irradiation.

Section 3. Crystal structure analysis of Co^{II}–W^{V} phase of RbCoW

Table S1. Crystallographic data and structure refinement of the Co^{II}–W^{V} phase of **RbCoW** at 300 K.

Compound	**RbCoW** (Co^{II}–W^{V} phase)
Empirical formula	$C_{20}H_8CoN_{12}RbW$
Formula weight	744.63
Temperature/K	300(2)
Crystal system	triclinic
Space group	$P\bar{1}$
a/Å	7.5298(4)
b/Å	13.7545(7)
c/Å	14.0687(6)
α/°	119.276(4)
β/°	101.020(6)
γ/°	89.974(6)
V/Å^3	1240.15(12)
Z	2
ρ_{calc}/g cm^{-3}	1.994
μ/mm^{-1}	7.286
F(000)	700.0
Crystal size/mm^3	0.204 × 0.042 × 0.024
Radiation	MoKα (λ = 0.71073)
2θ range for data collection/°	6.186 to 54.934
Index ranges	−9 ≤ h ≤ 9 −17 ≤ k ≤ 17 −18 ≤ l ≤ 18
Reflections collected	11945
Independent reflections	5621 [R_{int} = 0.0911, R_{sigma} = 0.1318]
Data/restraints/parameters	5621/23/256
Goodness-of-fit on F^2	1.140
Final R indexes	R_1 = 0.0829
[I>=2σ (I)]	wR_2 = 0.1260
Final R indexes	R_1 = 0.1152
[all data]	wR_2 = 0.1352
Largest diff. peak/hole / e Å^{-3}	2.10/−4.75

Section 4. First-principles phonon mode calculation

Table S2-1. Calculated optical phonon modes obtained by first-principles phonon mode calculations of **RbCoW**.

Frequency [THz]	Wavenumber [cm^{-1}]	Irreducible representation	Infrared intensity [×10^{-4}]	Frequency [THz]	Wavenumber [cm^{-1}]	Irreducible representation	Infrared intensity [×10^{-4}]	Frequency [THz]	Wavenumber [cm^{-1}]	Irreducible representation	Infrared intensity [×10^{-4}]
0.883	29.4	A_u	3.4880	4.182	139.4	A_u	2.5720	9.844	328.1	A_g	0.0000
0.997	33.2	A_u	13.9400	4.236	141.2	A_g	0.0000	9.994	333.1	A_u	7.5450
1.136	37.9	A_u	17.6050	4.374	145.8	A_g	0.0000	10.449	348.3	A_u	125.1880
1.166	38.9	A_g	0.0000	4.521	150.7	A_u	56.5530	10.492	349.7	A_g	0.0000
1.286	42.9	A_g	0.0000	4.523	150.8	A_g	0.0000	10.661	355.4	A_u	35.5870
1.453	48.4	A_u	8.2990	4.601	153.4	A_u	44.8030	10.681	356.0	A_g	0.0000
1.490	49.7	A_g	0.0000	4.708	156.9	A_g	0.0000	10.716	357.2	A_g	0.0000
1.571	52.4	A_g	0.0000	4.755	158.5	A_g	0.0000	10.759	358.6	A_u	4.5580
1.603	53.4	A_g	0.0000	4.830	161.0	A_u	71.1950	10.762	358.7	A_g	0.0000
1.682	56.1	A_u	10.0230	5.000	166.7	A_u	75.3830	10.768	358.9	A_u	2.6290
1.745	58.2	A_g	0.0000	5.081	169.4	A_g	0.0000	10.793	359.8	A_u	0.5130
1.805	60.2	A_u	4.6260	5.107	170.2	A_g	0.0000	10.950	365.0	A_g	0.0000
1.912	63.7	A_g	0.0000	5.113	170.4	A_u	354.8910	10.975	365.8	A_u	18.5100
1.923	64.1	A_u	3.2580	5.278	175.9	A_u	70.9100	11.129	371.0	A_u	30.4830
1.998	66.6	A_g	0.0000	5.418	180.6	A_u	33.8680	11.153	371.8	A_g	0.0000
2.102	70.1	A_u	30.1720	5.576	185.9	A_u	8.4450	11.313	377.1	A_g	0.0000
2.172	72.4	A_g	0.0000	5.602	186.7	A_u	30.5130	11.430	381.0	A_u	0.6020
2.188	72.9	A_u	0.1350	5.693	189.8	A_g	0.0000	11.692	389.7	A_g	0.0000
2.244	74.8	A_g	0.0000	5.788	192.9	A_u	0.9050	11.734	391.1	A_u	8.6860
2.341	78.0	A_g	0.0000	5.832	194.4	A_g	0.0000	11.748	391.6	A_g	0.0000
2.408	80.3	A_g	0.0000	5.879	196.0	A_u	0.6440	11.769	392.3	A_u	48.5640
2.484	82.8	A_u	2.8260	5.985	199.5	A_g	0.0000	11.988	399.6	A_g	0.0000
2.546	84.9	A_g	0.0000	6.042	201.4	A_g	0.0000	12.017	400.6	A_u	48.7900
2.569	85.6	A_u	6.1700	6.203	206.8	A_u	3.4400	12.148	404.9	A_g	0.0000
2.607	86.9	A_g	0.0000	6.246	208.2	A_u	2.8060	12.230	407.7	A_u	96.5540
2.657	88.6	A_u	17.8610	6.296	209.9	A_u	3.4540	12.287	409.6	A_g	0.0000
2.893	96.4	A_g	0.0000	6.379	212.6	A_g	0.0000	12.315	410.5	A_u	10.4700
2.962	98.7	A_u	0.8400	6.533	217.8	A_g	0.0000	12.387	412.9	A_g	0.0000
3.042	101.4	A_g	0.0000	6.563	218.8	A_u	0.2040	12.391	413.0	A_u	3.2700
3.047	101.6	A_u	4.2980	6.613	220.4	A_g	0.0000	12.586	419.5	A_u	3.1320
3.173	105.8	A_g	0.0000	6.617	220.6	A_u	0.4300	12.593	419.8	A_g	0.0000
3.284	109.5	A_u	0.0010	6.733	224.4	A_g	0.0000	12.780	426.0	A_g	0.0000
3.354	111.8	A_g	0.0000	7.006	233.5	A_u	176.0970	12.788	426.3	A_u	20.2580
3.367	112.2	A_u	1.7940	7.236	241.2	A_g	0.0000	12.890	429.7	A_g	0.0000
3.466	115.5	A_u	5.1640	7.307	243.6	A_u	57.2250	12.964	432.1	A_u	31.6900
3.481	116.0	A_u	2.4870	7.502	250.1	A_u	29.7720	12.977	432.6	A_g	0.0000
3.508	116.9	A_g	0.0000	7.623	254.1	A_u	0.2270	13.156	438.5	A_u	0.9030
3.566	118.9	A_g	0.0000	9.368	312.3	A_g	0.0000	13.191	439.7	A_g	0.0000
3.751	125.0	A_g	0.0000	9.485	316.2	A_u	2.1460	13.303	443.4	A_u	53.7610
3.948	131.6	A_u	0.1650	9.684	322.8	A_g	0.0000	13.359	445.3	A_g	0.0000
4.014	133.8	A_g	0.0000	9.745	324.8	A_g	0.0000	13.463	448.8	A_u	1.6350
4.097	136.6	A_u	1.9980	9.832	327.7	A_u	0.3220	13.493	449.8	A_g	0.0000

Table S2-2. Calculated optical phonon modes obtained by first-principles phonon mode calculations of **RbCoW**.

Frequency [THz]	Wavenumber [cm^{-1}]	Irreducible representation	Infrared intensity [$\times 10^{-4}$]	Frequency [THz]	Wavenumber [cm^{-1}]	Irreducible representation	Infrared intensity [$\times 10^{-4}$]	Frequency [THz]	Wavenumber [cm^{-1}]	Irreducible representation	Infrared intensity [$\times 10^{-4}$]
13.667	455.6	A_u	2.5030	28.479	949.3	A_g	0.0000	46.575	1552.5	A_u	21.9990
13.759	458.6	A_g	0.0000	28.528	950.9	A_u	3.2320	46.593	1553.1	A_g	0.0000
13.824	460.8	A_g	64.9270	29.536	984.5	A_g	0.0000	46.614	1553.8	A_u	3.3100
13.824	460.8	A_u	0.0010	29.564	985.5	A_u	0.4940	47.397	1579.9	A_g	0.0000
13.951	465.0	A_u	83.4780	30.051	1001.7	A_u	0.7200	47.400	1580.0	A_u	60.6630
14.036	467.9	A_g	0.0000	30.123	1004.1	A_g	0.0000	47.419	1580.6	A_u	10.6150
14.113	470.4	A_u	11.5030	30.454	1015.1	A_g	0.0000	47.450	1581.7	A_g	0.0000
14.126	470.9	A_g	0.0000	30.486	1016.2	A_u	0.1820	63.791	2126.4	A_u	583.2660
14.157	471.9	A_u	3.7790	30.641	1021.4	A_g	0.0000	63.875	2129.2	A_g	0.0000
14.201	473.4	A_g	0.0000	30.643	1021.4	A_u	0.1070	64.065	2135.5	A_u	85.2680
14.349	478.3	A_u	0.2710	31.416	1047.2	A_g	0.0000	64.093	2136.4	A_g	0.0000
14.528	484.3	A_u	34.8430	31.432	1047.7	A_u	18.3140	64.153	2138.4	A_g	0.0000
14.768	492.3	A_g	0.0000	31.446	1048.2	A_g	0.0000	64.215	2140.5	A_u	35.2770
16.520	550.7	A_u	20.3140	31.471	1049.0	A_u	79.9600	64.516	2150.5	A_u	1671.552
16.524	550.8	A_g	0.0000	33.390	1113.0	A_u	4.8130	64.655	2155.2	A_g	0.0000
16.651	555.0	A_u	0.4780	33.411	1113.7	A_g	0.0000	64.699	2156.6	A_u	332.9170
16.684	556.1	A_g	0.0000	33.494	1116.5	A_u	2.2470	64.739	2158.0	A_g	0.0000
16.717	557.2	A_u	20.0610	33.575	1119.2	A_g	0.0000	64.809	2160.3	A_u	152.2790
16.728	557.6	A_g	0.0000	35.731	1191.0	A_u	59.6980	64.887	2162.9	A_g	0.0000
16.816	560.5	A_g	0.0000	35.732	1191.1	A_g	0.0000	64.973	2165.8	A_u	92.6680
16.859	562.0	A_u	17.7180	35.753	1191.8	A_u	11.4290	65.150	2171.7	A_g	0.0000
19.264	642.1	A_g	0.0000	35.852	1195.1	A_g	0.0000	65.232	2174.4	A_u	7.5780
19.281	642.7	A_u	6.3830	36.097	1203.2	A_u	2.5860	65.236	2174.5	A_g	0.0000
19.287	642.9	A_g	0.0000	36.103	1203.4	A_g	0.0000	68.061	2268.7	A_g	0.0000
19.350	645.0	A_u	72.4030	36.161	1205.4	A_g	0.0000	68.067	2268.9	A_u	5.4740
20.552	685.1	A_g	0.0000	36.185	1206.2	A_u	0.4180	68.207	2273.6	A_u	0.1530
20.564	685.5	A_u	351.0870	38.585	1286.2	A_g	0.0000	68.231	2274.4	A_g	0.0000
20.628	687.6	A_g	0.0000	38.610	1287.0	A_u	0.4450	92.449	3081.6	A_g	0.0000
20.722	690.7	A_u	178.4790	38.692	1289.7	A_g	0.0000	92.508	3083.6	A_u	6.2680
23.684	789.5	A_g	0.0000	38.716	1290.5	A_u	0.1360	92.520	3084.0	A_g	0.0000
23.707	790.2	A_u	1.6890	39.531	1317.7	A_u	0.0220	92.520	3084.0	A_u	4.1160
23.723	790.8	A_g	0.0000	39.541	1318.0	A_g	0.0000	92.701	3090.0	A_u	33.0030
23.730	791.0	A_u	2.8170	39.610	1320.3	A_g	0.0000	92.739	3091.3	A_g	0.0000
24.002	800.1	A_u	118.9470	39.626	1320.9	A_u	0.4020	92.841	3094.7	A_g	0.0000
24.075	802.5	A_g	0.0000	42.077	1402.6	A_g	0.0000	92.845	3094.8	A_u	5.1740
24.429	814.3	A_g	0.0000	42.095	1403.2	A_u	7.5080	92.994	3099.8	A_u	1.1500
24.545	818.2	A_u	133.3730	42.098	1403.3	A_g	0.0000	92.997	3099.9	A_g	0.0000
27.084	902.8	A_u	71.2950	42.102	1403.4	A_u	3.5130	93.055	3101.8	A_g	0.0000
27.094	903.1	A_g	0.0000	43.811	1460.4	A_g	0.0000	93.061	3102.0	A_u	9.5130
27.129	904.3	A_g	0.0000	43.813	1460.4	A_u	0.0010	93.286	3109.5	A_u	1.9800
27.149	905.0	A_u	23.1170	43.869	1462.3	A_g	0.0000	93.289	3109.6	A_g	0.0000
28.238	941.3	A_u	3.2230	43.874	1462.5	A_u	0.0040	93.321	3110.7	A_g	0.0000
28.239	941.3	A_g	0.0000	46.568	1552.3	A_g	0.0000	93.329	3111.0	A_u	7.7770

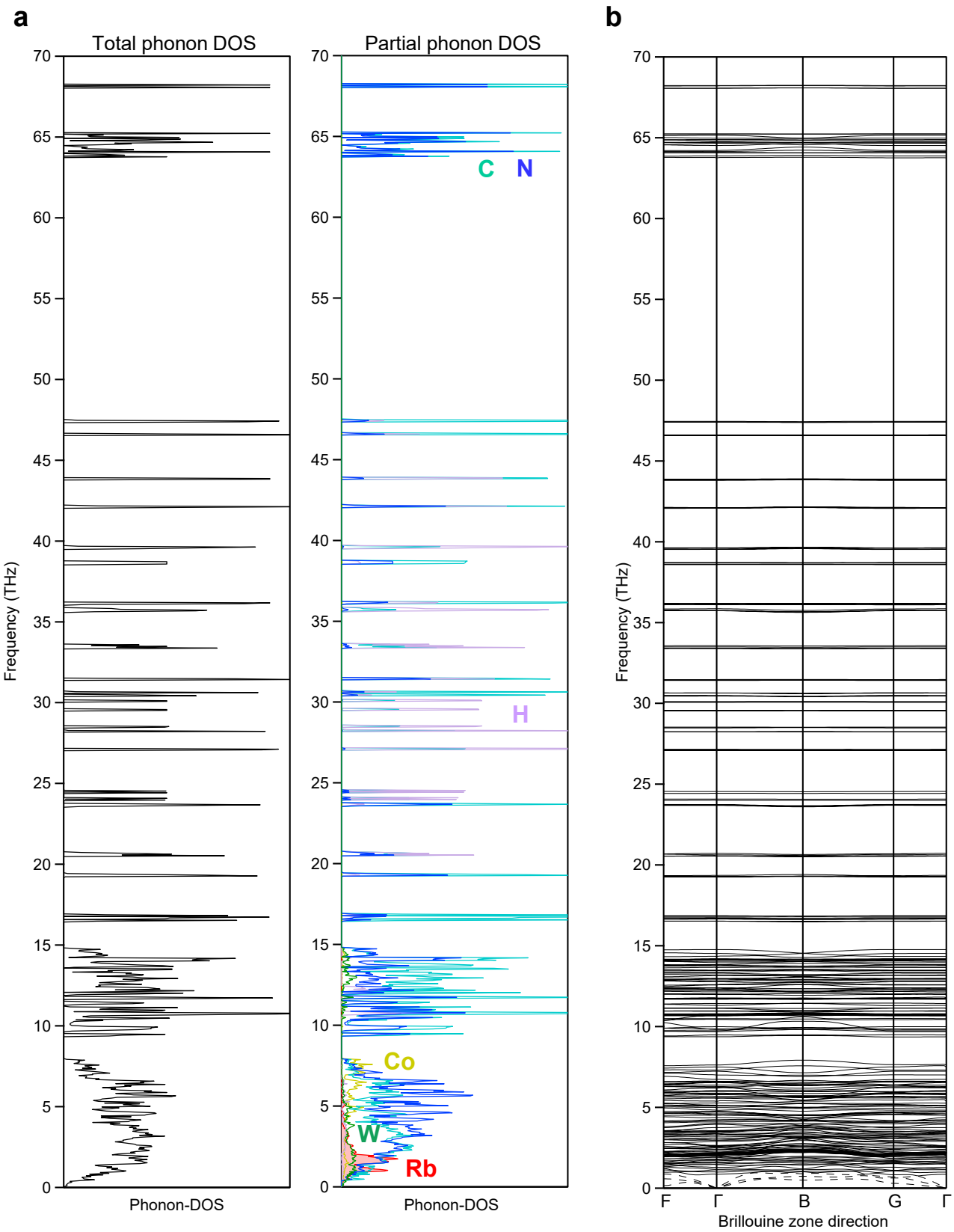

Figure S1. (a) Total phonon-DOS of the **RbCoW** Co^{II}–W^{V} phase (black line) and partial phonon-DOS of Rb (red line), Co (dark yellow line), W (green line), C (light blue line), N (blue line), and H (purple line). (b) Phonon dispersion of the **RbCoW** Co^{II}–W^{V} phase.

Table S3. Cell parameters of **RbCoW** before and after structural optimization, and their differences (Δ). Initial cell parameters before structural optimization are determined by single crystal structural analysis. Optimized cell parameters are used for the phonon mode calculations.

	Single crystal structural analysis	Optimized structure	Δ (%)
a / Å	15.060	15.026	−0.23
b / Å	13.755	13.728	−0.20
c / Å	14.069	14.036	−0.24
α / °	119.28	119.25	−0.03
β / °	101.02	100.97	−0.05
γ / °	89.97	90.00	0.03
V / Å^3	2480.3	2465.14	−0.61

Table S4. Atomic positions of **RbCoW** after structural optimization.

Atom label	x	y	z	Atom label	x	y	z	Atom label	x	y	z	Atom label	x	y	z
W	0.77481	0.82203	0.13874	N	0.22066	0.90475	0.67852	C	0.77374	0.16644	0.72228	C	0.15111	0.60754	0.33714
W	0.27481	0.82203	0.13874	N	0.53316	0.15481	0.15742	C	0.27374	0.16644	0.72228	C	0.84889	0.39246	0.66286
W	0.72519	0.17797	0.86126	N	0.03316	0.15481	0.15742	C	0.78007	0.0001	0.25702	C	0.34889	0.39246	0.66286
W	0.22519	0.17797	0.86126	N	0.96684	0.84519	0.84258	C	0.28007	0.0001	0.25702	C	0.62687	0.5509	0.21995
Rb	0.62245	0.06635	0.45143	N	0.46684	0.84519	0.84258	C	0.71993	0.9999	0.74298	C	0.12687	0.5509	0.21995
Rb	0.12245	0.06635	0.45143	N	0.80153	0.40764	0.40998	C	0.21993	0.9999	0.74298	C	0.87313	0.4491	0.78005
Rb	0.87755	0.93365	0.54857	N	0.30153	0.40764	0.40998	C	0.96433	0.20487	0.20596	C	0.37313	0.4491	0.78005
Rb	0.37755	0.93365	0.54857	N	0.69847	0.59236	0.59002	C	0.46433	0.20487	0.20596	C	0.74365	0.64868	0.39394
Co	0	0.5	0	N	0.19847	0.59236	0.59002	C	0.53567	0.79513	0.79404	C	0.24365	0.64868	0.39394
Co	0.5	0.5	0	N	0.53959	0.51809	0.16461	C	0.03567	0.79513	0.79404	C	0.75635	0.35132	0.60606
Co	0	0	0	N	0.03959	0.51809	0.16461	C	0.97872	0.30578	0.30673	C	0.25635	0.35132	0.60606
Co	0.5	0	0	N	0.96041	0.48191	0.83539	C	0.47872	0.30578	0.30673	H	0.89574	0.16216	0.1618
N	0.60417	0.62165	0.04534	N	0.46041	0.48191	0.83539	C	0.52128	0.69422	0.69327	H	0.39574	0.16216	0.1618
N	0.10417	0.62165	0.04534	N	0.81851	0.68573	0.4425	C	0.02128	0.69422	0.69327	H	0.60426	0.83784	0.8382
N	0.89583	0.37835	0.95466	N	0.31851	0.68573	0.4425	C	0.56734	0.35684	0.3597	H	0.10426	0.83784	0.8382
N	0.39583	0.37835	0.95466	N	0.68149	0.31427	0.5575	C	0.06734	0.35684	0.3597	H	0.92046	0.34364	0.34158
N	0.60168	0.93117	0.05601	N	0.18149	0.31427	0.5575	C	0.93266	0.64316	0.6403	H	0.42046	0.34364	0.34158
N	0.10168	0.93117	0.05601	C	0.66636	0.68975	0.07917	C	0.43266	0.64316	0.6403	H	0.57954	0.65636	0.65842
N	0.89832	0.06883	0.94399	C	0.16636	0.68975	0.07917	C	0.63888	0.30549	0.30816	H	0.07954	0.65636	0.65842
N	0.39832	0.06883	0.94399	C	0.83364	0.31025	0.92083	C	0.13888	0.30549	0.30816	H	0.58303	0.43545	0.43954
N	0.90872	0.61634	0.05768	C	0.33364	0.31025	0.92083	C	0.86112	0.69451	0.69184	H	0.08303	0.43545	0.43954
N	0.40872	0.61634	0.05768	C	0.66098	0.89122	0.08701	C	0.36112	0.69451	0.69184	H	0.91697	0.56455	0.56046
N	0.59128	0.38366	0.94232	C	0.16098	0.89122	0.08701	C	0.61903	0.20371	0.20647	H	0.41697	0.56455	0.56046
N	0.09128	0.38366	0.94232	C	0.83902	0.10878	0.91299	C	0.11903	0.20371	0.20647	H	0.67289	0.16123	0.16432
N	0.91108	0.94325	0.05887	C	0.33902	0.10878	0.91299	C	0.88097	0.79629	0.79353	H	0.17289	0.16123	0.16432
N	0.41108	0.94325	0.05887	C	0.85906	0.68566	0.08983	C	0.38097	0.79629	0.79353	H	0.82711	0.83877	0.83568
N	0.58892	0.05675	0.94113	C	0.35906	0.68566	0.08983	C	0.72971	0.35847	0.36112	H	0.32711	0.83877	0.83568
N	0.08892	0.05675	0.94113	C	0.64094	0.31434	0.91017	C	0.22971	0.35847	0.36112	H	0.9046	0.50052	0.17354
N	0.72952	0.67669	0.85972	C	0.14094	0.31434	0.91017	C	0.77029	0.64153	0.63888	H	0.4046	0.50052	0.17354
N	0.22952	0.67669	0.85972	C	0.86372	0.89968	0.08744	C	0.27029	0.64153	0.63888	H	0.5954	0.49948	0.82646
N	0.77048	0.32331	0.14028	C	0.36372	0.89968	0.08744	C	0.97428	0.53236	0.22279	H	0.0954	0.49948	0.82646
N	0.27048	0.32331	0.14028	C	0.63628	0.10032	0.91256	C	0.47428	0.53236	0.22279	H	0.93766	0.59867	0.38235
N	0.95812	0.89536	0.34534	C	0.13628	0.10032	0.91256	C	0.52572	0.46764	0.77721	H	0.43766	0.59867	0.38235
N	0.45812	0.89536	0.34534	C	0.74578	0.72962	0.95755	C	0.02572	0.46764	0.77721	H	0.56234	0.40133	0.61765
N	0.54188	0.10464	0.65466	C	0.24578	0.72962	0.95755	C	0.9933	0.58665	0.33919	H	0.06234	0.40133	0.61765
N	0.04188	0.10464	0.65466	C	0.75422	0.27038	0.04245	C	0.4933	0.58665	0.33919	H	0.60057	0.67687	0.48936
N	0.70362	0.84949	0.35927	C	0.25422	0.27038	0.04245	C	0.5067	0.41335	0.66081	H	0.10057	0.67687	0.48936
N	0.20362	0.84949	0.35927	C	0.89538	0.86757	0.27034	C	0.0067	0.41335	0.66081	H	0.89943	0.32313	0.51064
N	0.79638	0.15051	0.64073	C	0.39538	0.86757	0.27034	C	0.58257	0.62891	0.39815	H	0.39943	0.32313	0.51064
N	0.29638	0.15051	0.64073	C	0.60462	0.13243	0.72966	C	0.08257	0.62891	0.39815	H	0.67828	0.53426	0.1699
N	0.77934	0.09525	0.32148	C	0.10462	0.13243	0.72966	C	0.91743	0.37109	0.60185	H	0.17828	0.53426	0.1699
N	0.27934	0.09525	0.32148	C	0.72626	0.83356	0.27772	C	0.41743	0.37109	0.60185	H	0.82172	0.46574	0.8301
N	0.72066	0.90475	0.67852	C	0.22626	0.83356	0.27772	C	0.65111	0.60754	0.33714	H	0.32172	0.46574	0.8301

Section 5. Temperature-induced switching effect on the low-frequency phonon mode

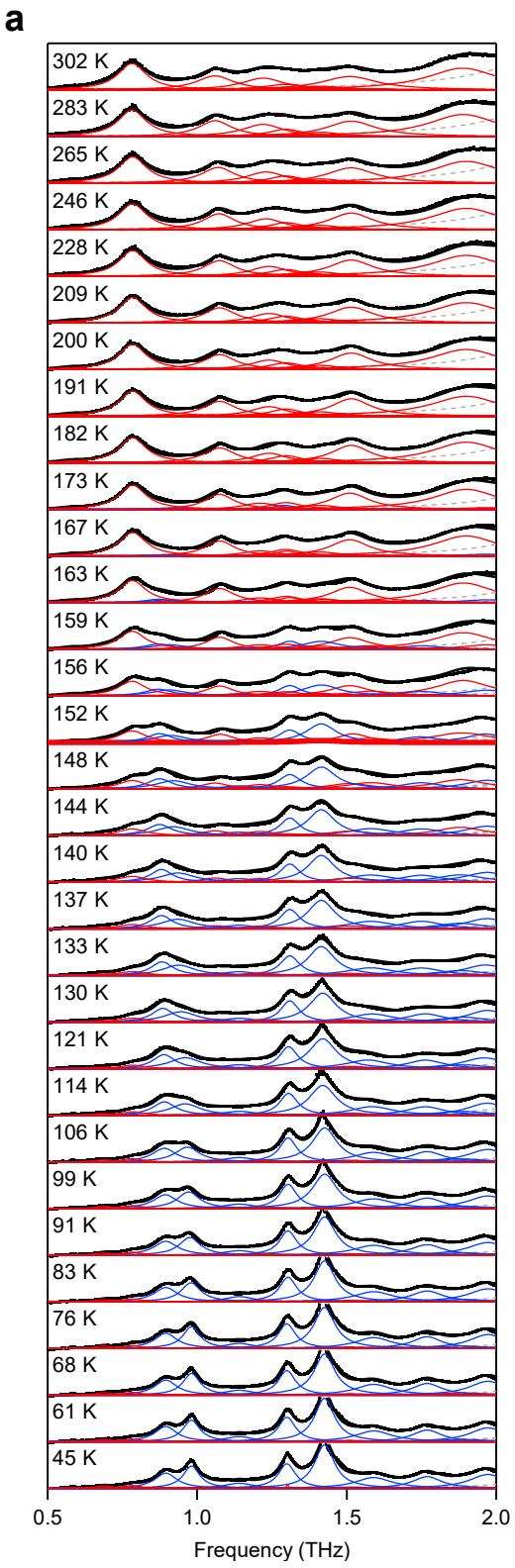

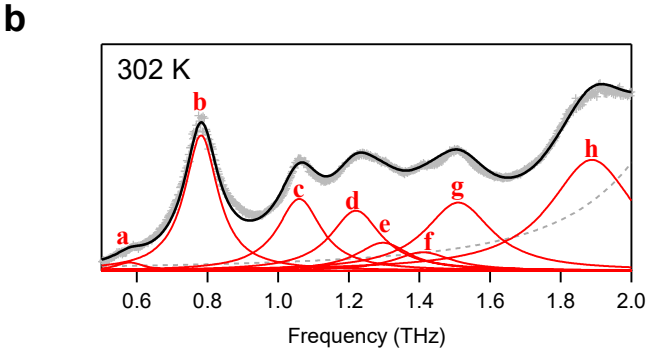

Co^{II}-W^{V} phase	a	b	c	d	e	f	g	h
Position (THz)	0.58	0.78	1.06	1.22	1.30	1.41	1.51	1.89
FWHM (THz)	0.10	0.12	0.15	0.18	0.19	0.20	0.23	0.29
Area	0.02	0.41	0.29	0.28	0.14	0.10	0.41	0.86

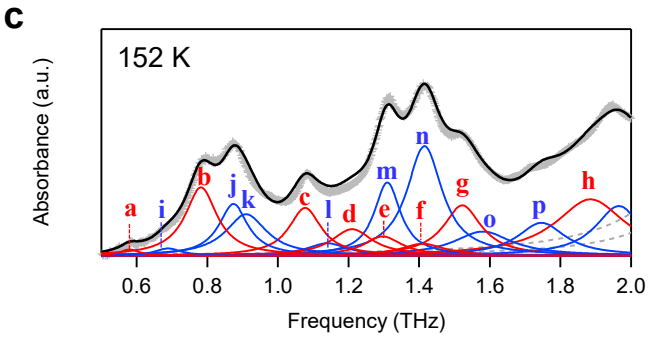

Co^{II}-W^{V} phase	a	b	c	d	e	f	g	h
Position (THz)	0.58	0.78	1.08	1.21	1.30	1.41	1.52	1.89
FWHM (THz)	0.07	0.11	0.11	0.14	0.13	0.15	0.13	0.24
Area	0.01	0.17	0.12	0.09	0.06	0.04	0.15	0.31

Co^{III}-W^{IV} phase	i	j	k	l	m	n	o	p
Position (THz)	0.69	0.87	0.91	1.14	1.31	1.42	1.58	1.75
FWHM (THz)	0.09	0.10	0.14	0.14	0.09	0.12	0.20	0.16
Area	0.01	0.12	0.13	0.04	0.15	0.31	0.11	0.12

Figure S2. (a) Peak analyses of the temperature-dependent THz absorption spectra. THz absorption spectra at (b) 302 K and (c) 152 K. Red lines, blue lines, and black lines indicate the peak components from the Co^{II}–W^{V} phase, those from the Co^{III}–W^{IV} phase, and the total calculated spectra of the Co^{II}–W^{V} and Co^{III}–W^{IV} phases, respectively. Grey dots show the experimental data. Faint dashed grey lines represent the fitted curve of the higher frequency phonon modes.

Section 6. Crystal structure analysis of the Co^{III}–W^{IV} phase of RbCoW

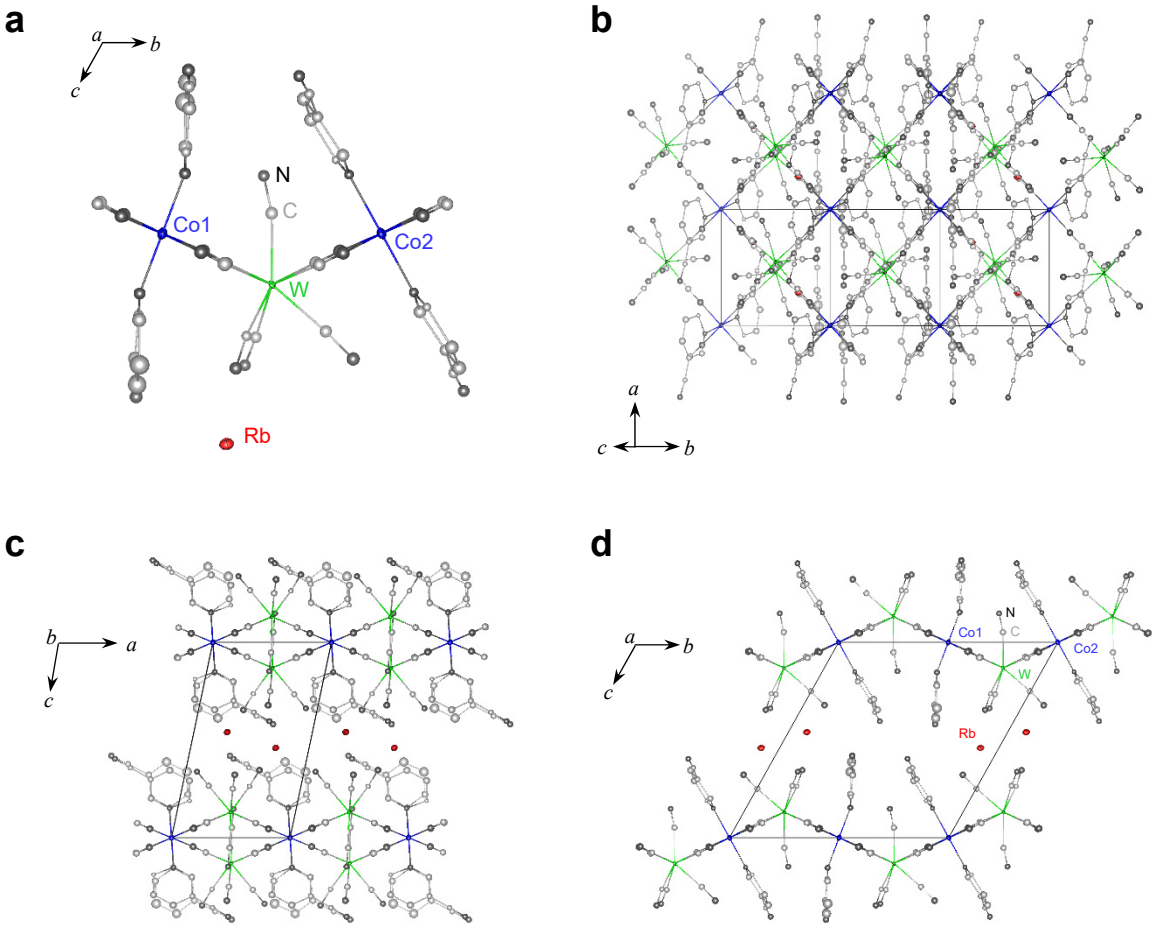

Figure S3. Crystal structure of the Co^{III}–W^{IV} phase of **RbCoW** at 130 K. (a) Coordination environment around the metal ions shown by 30 % probability thermal ellipsoids. (b) Crystal structure viewed along the *c*-axis, (c) *b*-axis, and (d) *a*-axis. Red, blue, pale green, grey, and black balls represent Rb, Co, W, C, and N atoms, respectively. Hydrogen atoms are omitted for clarity.

Table S5. Crystallographic data and structure refinement of the Co^{III}–W^{IV} phase of **RbCoW** at 130 K.

Compound	RbCoW (Co^{III}–W^{IV} phase)
Empirical formula	$C_{20}H_8CoN_{12}RbW$
Formula weight	744.63
Temperature/K	130(2)
Crystal system	triclinic
Space group	$P\bar{1}$
a/Å	7.2253(14)
b/Å	13.340(3)
c/Å	13.839(3)
α/°	118.671(8)
β/°	100.497(7)
γ/°	90.100(6)
V/Å^3	1144.6(4)
Z	2
ρ_{calc}/g cm^{-3}	2.161
μ/mm^{-1}	7.895
F(000)	700.0
Crystal size/mm^3	0.204 × 0.042 × 0.024
Radiation	MoKα (λ = 0.71075)
2θ range for data collection/°	5.978 to 54.952
Index ranges	$-9 \le h \le 9$ $-17 \le k \le 17$ $-15 \le l \le 17$
Reflections collected	10853
Independent reflections	5234 [R_{int} = 0.1070, R_{sigma} = 0.1500]
Data/restraints/parameters	5234/23/256
Goodness-of-fit on F^2	1.172
Final R indexes	R_1 = 0.1105
[I>=2σ (I)]	wR_2 = 0.1690
Final R indexes	R_1 = 0.1424
[all data]	wR_2 = 0.1797
Largest diff. peak/hole / e Å^{-3}	3.35/−5.70

Section 7. Comparison of the crystal structure of RbCoW between the Co^{II}–W^{V} phase and Co^{III}–W^{IV} phase

Table S6. Comparison of the bond lengths (W–C and Co–N) and bond angles (∠Co–N– C (3-CNpy)) of **RbCoW** between the Co^{II}–W^{V} phase (300 K) and Co^{III}–W^{IV} phase (130 K).

	Co^{II}–W^{V} phase	Co^{III}–W^{IV} phase
Temperature	300	130
W1–C1	2.139(13)	2.145(19)
W1–C2	2.129(14)	2.136(19)
W1–C3	2.135(13)	2.150(14)
W1–C4	2.144(13)	2.138(18)
W1–C5	2.173(19)	2.16(3)
W1–C6	2.153(14)	2.19(3)
W1–C7	2.146(16)	2.181(19)
W1–C8	2.155(18)	2.17(3)
Ave. W–C	2.15(13)	2.16(19)
Co1–N2	2.080(11)	1.878(14)
Co1–N3	2.092(12)	1.882(14)
Co1–N9	2.164(18)	2.00(5)
Co2–N1	2.084(11)	1.876(13)
Co2–N4	2.099(12)	1.902(14)
Co2–N11	2.14(3)	1.88(4)
Ave. Co–N	2.11(2)	1.90(3)
∠Co1 – N9 – C11(3-CNpy)	178.1(5)	174.8(5)
∠Co2 – N11 – C17(3-CNpy)	156.2(4)	163.2(5)

Table S7. List of atomic distances between the Rb ion and the surrounding atoms.

	Co^{II}–W^{V} phase	Co^{III}–W^{IV} phase
Rb–N5	3.146(19)	3.04(3)
Rb–C5	3.68(2)	3.55(4)
Rb–N7	3.14(2)	3.07(3)
Rb–C7	3.697(19)	3.58(3)
Rb–N12	2.989(18)	3.03(3)
Rb–C20	3.551(15)	3.55(3)
Rb–N5’	3.64(2)	3.62(3)
Rb–C5’	4.301(17)	4.34(3)
Rb–N6’	3.235(18)	3.20(3)
Rb–C6’	3.63(3)	3.60(4)
Rb–N7’	3.05(2)	2.947(18)
Rb–C7’	3.502(13)	3.468(18)

Section 8. First-principles electronic structure calculation of the Co^{III}–W^{IV} phase

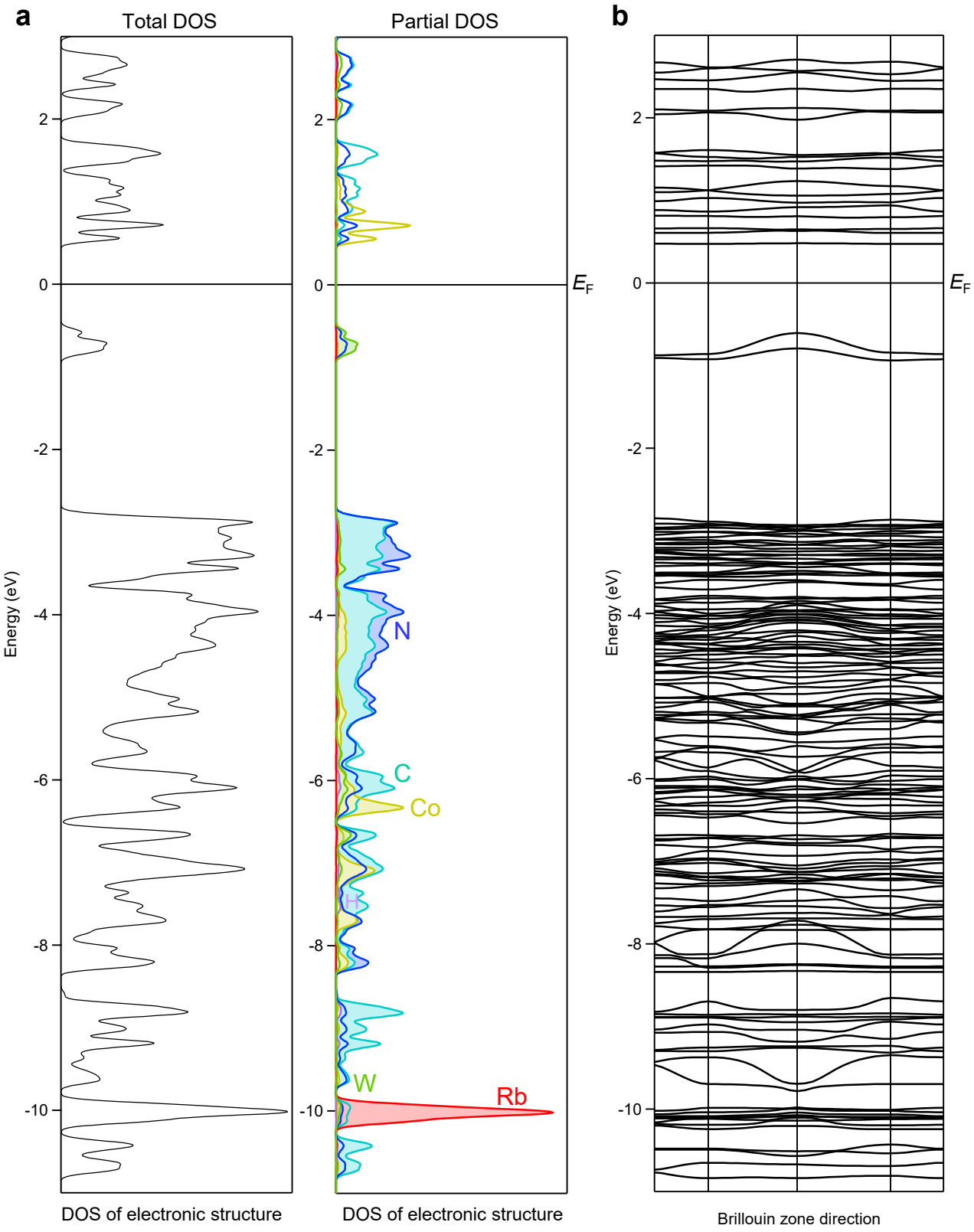

Figure S4. (a) Total DOS of the Co^{III}–W^{IV} phase (black line) and partial phonon DOS of Rb (red line), Co (dark yellow line), W (green line), C (light blue line), N (blue line), and H (purple line). (b) Band structure of the Co^{III}–W^{IV} phase of **RbCoW**.

Section 9. THz absorption spectrum of CsCoW

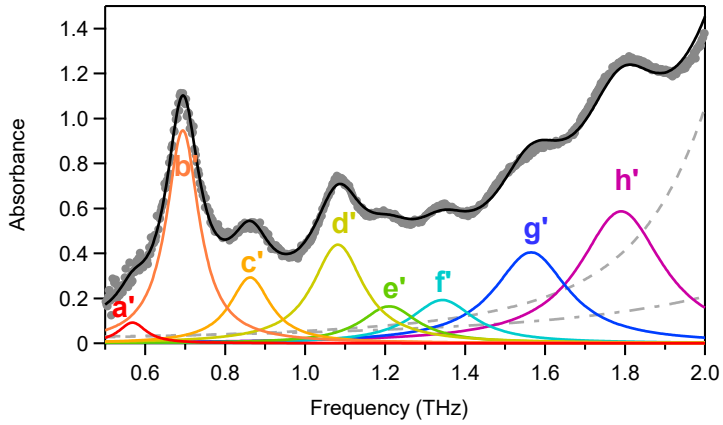

	a'	b'	c'	d'	e'	f'	g'	h'
Position (THz)	0.57	0.69	0.86	1.08	1.21	1.34	1.57	1.79
FWHM (THz)	0.08	0.10	0.12	0.16	0.17	0.19	0.23	0.25
Area	0.01	0.15	0.06	0.11	0.04	0.06	0.14	0.23

Figure S5. THz absorption spectrum of $Cs[Co^{II}(3\text{-cyanopyridine})_2][W^{V}(CN)_8]$ (**CsCoW**) with peaks at 0.57 (peak a'), 0.69 (peak b'), 0.86 (peak c'), 1.08 (peak d'), 1.21 (peak e'), 1.34 (peak f'), 1.57 (peak g'), and 1.79 THz (peak h'). Grey dots show the experimental data measured at room temperature, black line shows the fitted spectrum, and coloured lines indicate the components of each peak. Faint dashed grey lines represent the fitted curves of the higher frequency phonon modes.